Uniport Journal of Engineering and Scientific Research (UJESR)

Vol. 8, Issue 2, 2024, Page 101-120
ISSN: 2616-1192

(www.ujesr.org)

An Efficient Bathymetric Assessment of Erelu reservoir for its sustainability

Shittu, I.O[1*], Olorunkosebi, H.O[1], Hamid-Mosaku, A.I[2], Jimoh, O.A[2], Akindiya, O.M[1], Oyelakin, L.O[1], Muhammed, L.O[3], Raheem, K.A[4]

[1]Department of Surveying and Geoinformatics, Federal School of Surveying, Oyo State, Nigeria.
[2]Department of Surveying and Geoinformatics, University of Lagos, Lagos State, Nigeria.
[3]Al-Thaomein Survey Services, Oyo State, Nigeria.
[4]Department of Civil & Environmental Engineering, University of Port Harcourt, Choba, Port Harcourt, Rivers State, Nigeria.
*Corresponding author's email: oyekesinro@gmail.com

Abstract
Erelu reservoir plays a crucial role in supplying domestic water and supporting fisheries. However, there is a lack of documented initial design, depth information and proper maintenance, leading to issues such as overgrown aquatic weeds, sediment build-up, and human activities harming the reservoir. It is important to regularly assess its operational and environmental status to ensure its sustainability. This study evaluated the current geospatial condition of the reservoir using satellite images, depth measurements, and GNSS positional data. The research found that the minimum and maximum depths are 0.36m and 5.69m, with an average depth of 2.52m. Additionally, the reservoir has lost approximately 67 hectares of its original coverage, and its current volume is measured at 2,262,783.486 cubic meters. The research suggests that the reservoir is shallow and recommends thorough dredging as a remedial measure.

Keywords: *Reservoir, Sounding, Geospatial, Aquatic weeds, Sediment, Dredging*

Received: 9th June, 2024 *Accepted: 17th September, 2024*

1. Introduction

Erelu reservoir has been a vital source of domestic water supply for the people of Oyo and neighbouring towns for many years. In addition to providing water, it supports activities such as fish production, agriculture, and flood control. The reservoir was created in 1961 through the damming of the Awon River and has since been supplemented by various tributaries including Isuwin, Oroki, Ogbagba, Oloro, Elesin, and Abata (Kareem, 2016; Kareem *et al*., 2018; Kareem *et al*., 2015). Regular inspection and maintenance are crucial to prevent failure, which could lead to loss of life and property (Kareem et al., 2015).

Researchers, referencing sources such as Ayoola and Ajani (2009), Falaye *et al*. (2015), Jenyo-Oni *et al*. (2014), Kareem (2016), Kareem *et al*. (2018), Kareem *et al*. (2015), Olanrewaju *et al*. (2017), Popoola *et al*. (2019), have extensively studied Erelu and other reservoirs in the same geographical area. They have focused on physio-chemical attributes, distribution of fauna and flora, trace metal accumulation, abundance of plankton and benthic macroinvertebrates, spatial and temporal limnological status. However, there has been a lack of attention to bathymetric mapping of Erelu reservoir. Therefore, it is necessary to investigate and map the riverbed morphology, generate bathymetric charts, and carry out spatial analyses to effectively develop response strategies and engage in thorough planning processes.

Bathymetric information is a crucial part of hydrographic data (Kim *et al*., 2020; Kopacz *et al*., 1996) and is important for various purposes such as ensuring safe navigation, calculating water volume, managing pollution, supporting mineral and fish industries, facilitating underwater engineering construction, and aiding in the planning, construction, and maintenance of harbours and docks (Elhassan, 2015). The actual depth status of the Erelu reservoir, which was impounded in 1961, is currently unknown. Having accurate information about the reservoir's depth and potential underwater hazards is essential for conducting volumetric assessments, area evaluations, and riverbed profile examinations. Additionally, this information assists anglers and researchers in identifying optimal habitats for fish and other aquatic species for feeding, dwelling, and breeding.

Based on observations and interviews with local residents, it is evident that the water level of the reservoir changes with the seasons and the depth decreases over time, particularly during the dry season. This decline may be influenced by inflowing tributaries, erosion carrying sediments, and seasonal variations, which affect the riverbed morphology. Alademomi (2017) identified various factors that determine the morphology and hydrodynamic characteristics of coastal waters, including size, prevailing seasonal conditions, and human activity.

Several bathymetric approaches have been used by researchers, including the conventional lead-line approach, underwater Single-beam and Multibeam sonar approaches, satellite-based radar, and aircraft-based LiDAR approach. In this study, the Single-beam Echosounder approach was chosen due to its extensive history, minimal risk profile, and widespread acceptance. This method involves using a single-beam instrument mounted on a survey vessel in conjunction with a GNSS receiver to collect three-dimensional data points representing spatial coordinates (x, y, and z). While this method is known to be labour-intensive and demanding of skilled professionals, it is commonly used in shallow water environments where the time required to achieve 100% bathymetric coverage is high or beyond the client's budget compared to Multibeam sonar. The Single-beam Echosounder approach revolutionizes hydrographic surveying by using sound pulses to indirectly determine the depth from the water surface to the seafloor. To ensure precise measurements, proper calibration of the sounder is essential to account for variations in water properties such as type, salinity levels, temperature, and other factors that influence the speed at which sound waves propagate through the water column.

When conducting underwater topographic surveys, it is customary to position survey lines at right angles to the underwater slopes. The distance between these parallel survey lines depends on the intended scale and resolution of the final output. Additionally, tie lines, also referred to as longitudinal lines, are established perpendicular to the main survey lines but at greater intervals. These tie lines serve a dual purpose by providing a supplementary check on the accuracy of the collected field data and ensuring a robust quality assurance mechanism within the survey framework. The single-beam echo sounder remains the most common tool used in port and harbour surveys, providing valid results when used correctly in a well-planned and executed survey (FIG, 2010).

Despite technological advancements, single-beam echo sounders also offer some advantages over Multibeam Echosounder system (MBES) surveys and LiDAR technology. Compared to the single-beam approach, both LiDAR and MBES are typically expensive to operate as they gather millions of points within a short time frame. Although LiDAR technology has high capability in penetrating water columns to collect seafloor data, it is still challenging to acquire precise and high-resolution seafloor depths from space (Breman and Kearns, 2010). Additionally, data observed in an MBES system often include outliers (inconsistent or atypical values) due to the complexity of the acquisition process, potentially affecting up to 25% of the obtained data, depending on the sensor characteristics and environmental conditions (Le Deunf et al., 2020; Santos et al., 2017). However, single-beam data cannot be entirely free from spikes. The primary limitation associated with Single Beam Echo Sounder (SBES) is its capability to illuminate only a limited section of the seafloor, which results in the exclusion of bathymetric data between survey lines. In contrast, Multibeam Echo Sounders (MBES) offer the advantage of providing uninterrupted coverage (Šiljeg et al., 2022). Therefore, conducting comprehensive surveys in coastal areas requires a significant investment of time and resources to cover relatively small segments of the seafloor (Dierssen, 2014; Dierssen and Randolph, 2011).

This research focuses on the bathymetric mapping of Erelu reservoir using a single-beam Echo sounder approach. As a multipurpose reservoir providing potable and irrigation water for the province of Oyo and its catchment area, it is important to determine the depth status for effective management. This information is crucial for properly allocating water for domestic and irrigation use, as well as for proper future planning and sustainable management of the area.

2. Materials and methods

2.1 Study area

Erelu Reservoir (Fig. 1) lies in the south-western region of Nigeria between 598036mE- 601036mE and 870632mN- 874232mN, geographically referenced to WGS-1984 / UTM Zone 31N. The region is marked by a tropical savannah climate, exhibiting two clearly defined seasons, namely wet and dry, spanning from April to October and November to March correspondingly. The average yearly temperature hovers around 27°C, with an average annual precipitation of approximately 591.6 mm (Falaye et al., 2015). The reservoir, established through the impoundment of the Awon River in 1961, spans approximately 315.86 square kilometres in catchment area and covers 161.07 hectares in surface area. It is linked to various tributaries including Isuwin, Oroki, Ogbagba, Oloro, Elesin, Awon, and Abata. Additionally, secondary activities conducted within the vicinity encompass lowland agricultural practices along its perimeters, irrigation of arable crops by local farmers, gracing of animals to the area, particularly by fishermen (Kareem, 2016). It has normal periods of oscillation which make them relatively unresponsive to either the diurnal or semi diurnal forces. Thus, there are no measurable tides in the water, but it experiences a tidal stream.

It is important to clarify that the area in question refers specifically to the section of the Erelu body that remains free from aquatic weeds, has not been inundated with sediments, and has not been repurposed for other uses. This definition does not pertain to the original dimensions of the waterbody.

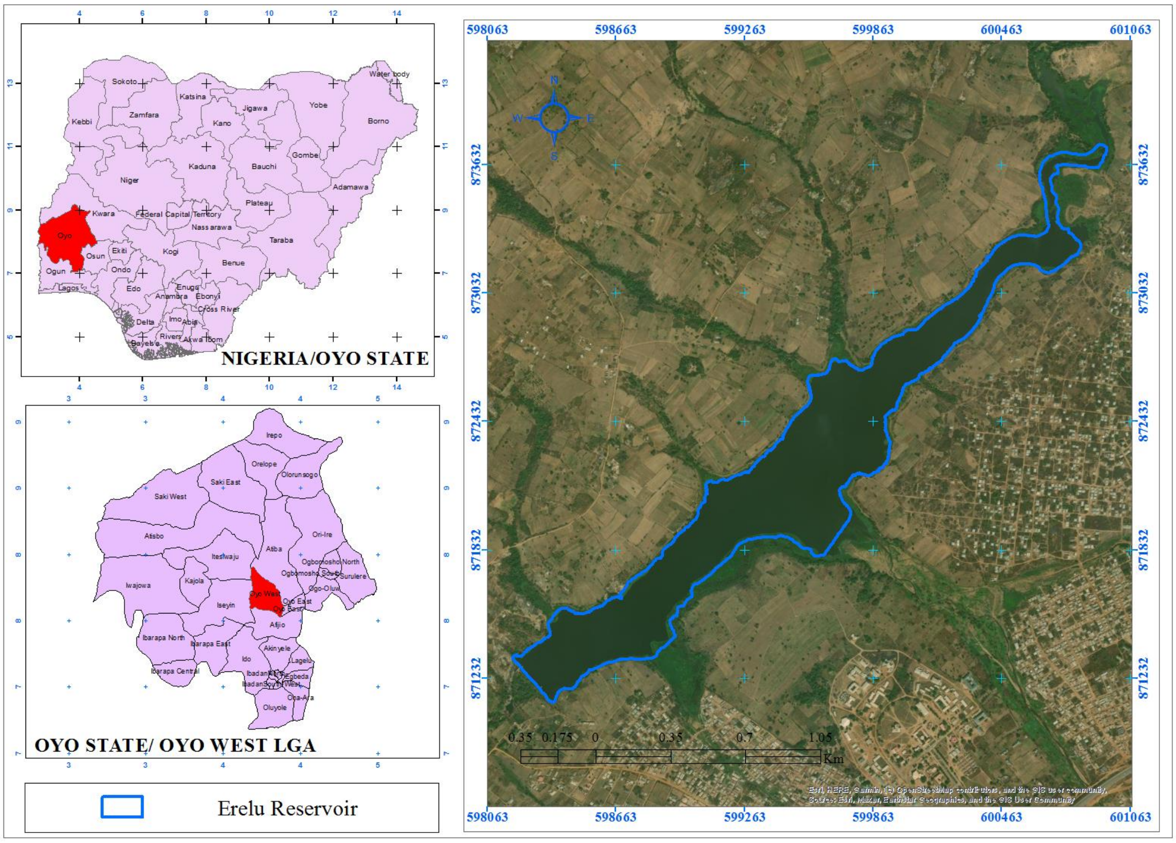

Fig. 1: Erelu reservoir (February, 2022)

2.2 Methodology

The methodology employed for assessing bathymetric information of Erelu Reservoir encompasses several sequential phases, as schematically shown in Fig. 2. These phases are further detailed in the subsequent subsections to provide a comprehensive overview of the methodological procedures and processing stages prior to presenting the results and findings.

2.2.1 Data source

Based on the initial study and consultations with various individuals in the study area, it was determined that no bathymetric observation has been conducted on the Erelu Reservoir. It was also noted that the water is non-tidal, although measurements to confirm this show that daily seasonal variations in the water level are minimal, indicating the absence of tides. The selection of data in the study (refer to Table 1) was influenced by the cost of acquisition and the choice of instruments. Consequently, specific data types were chosen to fulfil the research objectives.

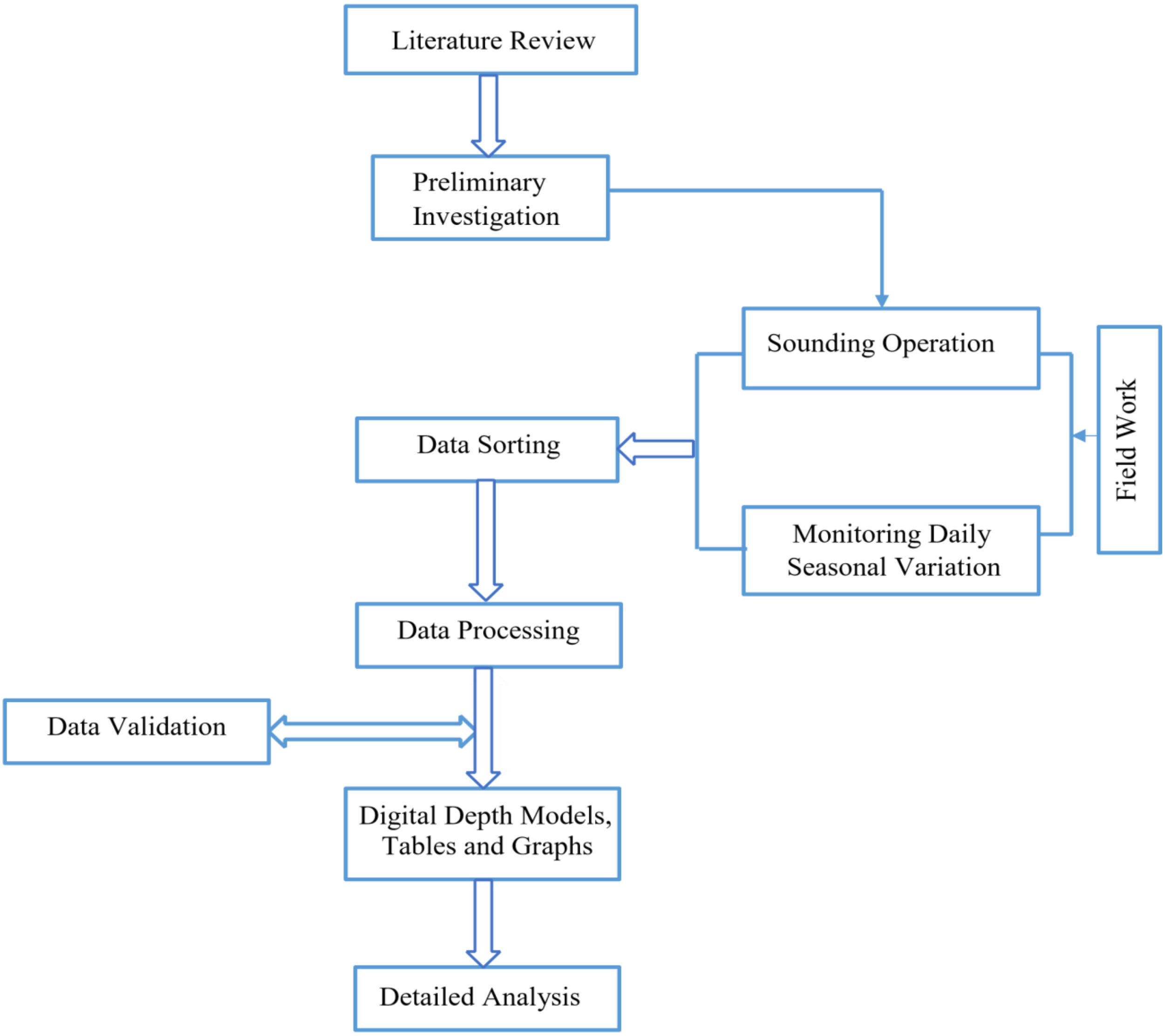

Fig. 2: Research workflow processes

Table 1: Data used and data source

S/N	Data type	Source	Date
1.	Water Boundary	Google earth Satellite Imagery	2022
2.	Sounding depth(s)	Authors	February, 2022

Google Earth satellite imagery was used to outline water boundaries in the study area using the ArcGIS "Editor Tool". This imagery also served as the base map for our reconnaissance and survey operations. Coordinated shoreline controls were established and used to orthorectify the imagery. The coordinates, observed with South Galaxy G1 GNSS receivers, were used to check the accuracy of corresponding points on the imagery. Additionally, the digitized map illustrates the reservoir's geometry.

2.2.2 Data acquisition

The data collection process entailed two distinct methodologies: sounding operation and monitoring daily seasonal variations of the water level; and described as follows.

2.2.2.1 Sounding operation

The sounding operation involves using Echosounder equipment to determine the depth of the riverbed. This is done by emitting ultrasonic waves from the Echosounder's transducers, which then get reflected and refracted off the river bottom.

A part of this signal is received by a receiver on the transmitting vessel, and the data is recorded to calculate the depth based on the time taken for the signal to travel back and forth and the known sound velocity in water.

To install the transducer, it was fixed to the transducer junction pole while the pole was passed through an iron bracket holder after the cable had been passed through it. The notch of the transducer was aligned with the screw hole of the junction pole and then secured with a metal screw. The transducer was then immersed in the water, ensuring it was parallel to the measuring boat. The draft value, which is the measurement value from the bottom of the transducer to the surface of the water, was then measured.

The GNSS receiver was installed directly above the transducer junction pole and connected to the SDE 28S+ Echosounder for planimetric positioning. The transducer cable was connected to the internal port of the Echosounder, and the power source cable was connected to power on the instrument.

The SDE-230 program was launched on the Echosounder, and the auto button was clicked to activate the echo-sounder into auto measuring mode. During this time, the transducer emitted an acoustic signal. Various parameters such as the draft value and sound velocity were inputted on the settings module after performing a proper bar check test with an allowable uncertainty of ±0.04m. The accurate measurement of the draft value was carefully observed.

Bar checks are essential for correcting velocity variations, draft variations, and index errors in the echo-sounding system. The bar check calibration measures the effect of varying sound propagation velocity. It involves a reflective bar or plate lowered beneath the transducer on marked lines at various depths (refer to Fig. 3).

During the bar check, a series of depth intervals were observed, down to the project depth. The observed depths were compared with the known depths marked on the lowering bar or plate, and the necessary corrections for sound propagation velocity were computed by comparing the observed depths against the known depths on the plate or bar.

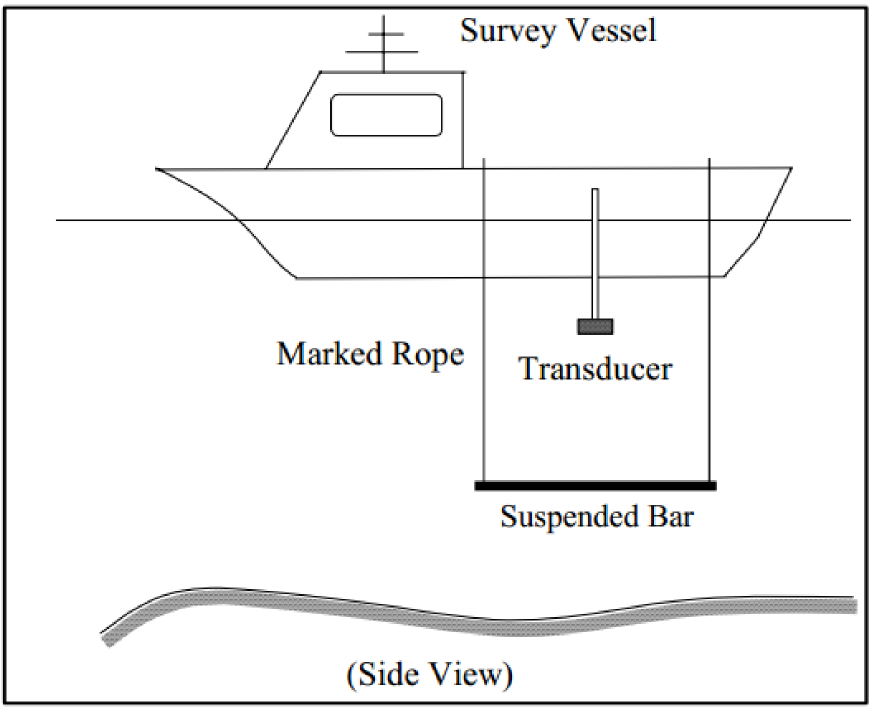

Fig. 3: Schematic depiction of bar check calibration

Following the previous steps, the record button was pressed to start recording the depths. Subsequently, the second software, PowerNAV, was launched to acquire planimetric position for the depths. Geodetic parameters were set as WGS 1984 UTM Zone 31N with a central meridian of 3. The connecting button was then pressed to integrate all the hardware, and the start button was clicked to initiate the sounding operation. The survey vessel maintained a constant speed during data capture.

The Echosounder was set to capture data at 30 second intervals. Bar checks were regularly conducted during the survey operations and at the end of each day's survey to ensure data accuracy. All other necessary precautions were taken before leaving the site while the estimation of reservoir perimeter using the digitized map was not left out. At shallow areas with depths less than the draft values (i.e., 0.5m), the direct method of sounding (using a levelling staff) was employed, especially in rocky and weedy areas.

2.2.2.2 Daily seasonal variation monitoring

The water level's daily seasonal variation was monitored to demonstrate how it changes over time. A levelling staff, held vertically with a pole tied to it, was set up in the water at a specific location where the markings could be read easily. The water level was recorded every 10 minutes, starting before the sounding operation and ending immediately after the sounding operation concluded.

2.2.3 Data processing

2.2.3.1 Data cleaning

When the survey boat was moving across the water's surface to collect depth readings, noise could interfere with the data collected by the Echosounder. This noise could come from false echoes or errors in the Echosounder. However, the noise was removed, and the usable data was sorted and downloaded from the Echosounder's Display Unit. The depth readings and the positional data from the GNSS receiver, were stored in the Echosounder's onboard computer display memory. After removing the noises and deleting unusable data, the cleaned information was opened with Microsoft Excel. The complete sounding data, including positional and time information, were accessed and saved for further processing.

2.2.3.2 Sounding data reduction

The hydrographic sounding data collected in the field is typically adjusted to a standard reference plane by subtracting the tidal value at the time of observation. For non-tidal water, the sounding data is usually adjusted to either the long observed mean low water (I.H.O, 2005) or Mean Sea Level (MSL) (Britain, 1970). In engineering work, sounding data can be adjusted to the Land Levelling Datum (LLD), but this is not within the scope of this work.

For this specific work, the tidal range is minimal (see Appendix 1) and does not significantly affect the sounding operation. Therefore, the removal of tidal effect from the sounding data was not considered necessary. However, tying the depths to a nearby benchmark may be needed when determining the height of the riverbed for sedimentation analysis, engineering purposes, and similar applications; consequently, water level was determined prior to the sounding operation enabling its utility for future analyses. In the case of tidal water, it is mandatory to observe tides and tie the adopted reference level to a nearby benchmark.

2.2.3.3 Bathymetric quality control

The term quality control refers to the procedures put in place to ensure the quality and accuracy of data being collected using the chosen methodologies for a particular study. For this study, the data quality of the survey was ensured by calibrating the Echosounder (which was satisfactory before sounding) and calculating the vertical and horizontal uncertainties. The information necessary for computing uncertainties in depth for vertical and horizontal as provided by IHO S-44 (Appendix 2) is as follows:

$$TVU = \pm\sqrt{a^2 + (b \times d)^2} \quad (1)$$

$$THU = 5\text{m} + 5\% \text{ of depth} \quad (2)$$

where a signifies the portion of uncertainty that is invariant with depth, b is a coefficient which represents that portion of the uncertainty that varies with the depth, d represents the depth obtained and $b\ x\ d$ represents the portion of uncertainty that varies with the depth.

Order 1b was considered because the maximum depth for this work was 5.69m (shallower than 100m), indicating that underkeel clearance is not an issue (Belmonte, 2020) since no ships or vessels require underkeel clearance, as it is a contained body of water, not a navigable waterway. The study area's bottom characteristics suggest a low likelihood of underwater features being a threat to the working boat in the area. While the water is not part of the navigational system, it was categorized to a specific order, similar to the categorization used in land surveying. Moreover, Order 1b is suitable for applications such as water resource management (e.g. monitoring water levels, volume and quality), environmental monitoring (e.g. tracking sedimentation, aquatic life or water temperature) or engineering projects (e.g. dam maintenance, water intake structures or shoreline development). These examples are common purposes for bathymetric purposes in reservoirs despite the TVU values close to Special Order (Table 2) but not considered due its description (Appendix 2).

Table 2: The total vertical and horizontal uncertainties (at 95% confidence level)

Total Vertical Uncertainties (TVU)					
	Depth	**Order 2**	**Order 1a and 1b**	**Special order**	**Exclusive Order**
Based on IHO-S44 specifications	Average	1.001680786	0.501073674	0.25071447	0.151187782
	Maximum	1.008527123	0.505441946	0.253616158	0.155952415
Authors	TVU = ±0.263620564				

From Table 2, it was concluded that Total Vertical Uncertainty (TVU) value of ±0.263620564m is relatively low, thus indicates a high degree of depth in depth predictions that will also aid further evaluation and decision making. The model's predictions can be trusted within 0.26m of the true depth, which is a relatively small margin of error.

The formula adopted by the authors are as follows:

$$\text{Standard deviation(s)} = \sqrt{\frac{\sum_{i=1}^{n}(d_i - \bar{d})^2}{n-1}} \quad (3)$$

where d_i *is the depth point*, $\bar{d}$ *is the Average depth, and* n is the number of data points.

$$\text{Standard Error (SE)} = \frac{s}{\sqrt{n}} \quad (4)$$

$$TVU_{95\%} = \pm SE \times Z_\alpha \quad (5)$$

For 95% confidence level; $Z_\alpha = 1.96$

Total Horizontal Uncertainty (THU) is given by IHO as: 5m + 5% of depth, this implies that: THU = 5m + 5/100 * 5.69m = 5m + (0.2845) at 95% confidence level. It is clear from the provided TVU uncertainties for a bathymetric survey of an Order 1 Survey, which is ≤1.39 m (Ojinnaka, 2007), that the depth accuracy was within the IHO specifications. Different factors contributing to the vertical uncertainty are vertical datum errors, vertical positioning systems errors, Instrumental errors, errors in speed sound, vertical datum separation model errors, vessel motion errors, vessel draughts, vessel settlement and squat, and seafloor slope. In this work, the uncertainty is most likely associated with instrumental errors, and errors in the speed of sound.

2.2.3.4 Data cross validation in Surfer

Cross validation was used to assess the spatial variation in gridding quality and guide data sampling. It was performed on the linear Z values, not the transformed Z values. From the known values in the original data set, cross validation assesses the relative quality of the grid by computing and investigating the gridding errors (Table 3). In Surfer 16, these errors are calculated by removing the first observation from the data set, and using the remaining data and the specified algorithm to interpolate a value at the first observation location. Using the known observation value at this location, the interpolation error was computed as:

$$\textit{Error} = \textit{Interpolated value} - \textit{Observed value} \quad (6)$$

First, the initial observation was added back into the data set, and the second observation was excluded. With the remaining data (including the first observation) and the specified algorithm, a value was interpolated at the location of the second observation. The interpolation error was then calculated using the known observation value at this location. This process was repeated for the third, fourth, fifth observations, and so on, until all observations were all included. This procedure resulted in the generation of n interpolation errors.

Table 3: Data cross validation report

S/N	X	Y	Z	ID	Estimate	Residual	nData	ID Label
1	598311.46	871194.53	3.28	8	3.286464	0.006464	38	A
2	598388.53	871453.73	1.94	89	1.777828	-0.16217	49	B
3	598481.4	871498.45	2.8	138	2.613383	-0.18662	55	C
4	598708.63	871459.82	4.72	213	4.616734	-0.10327	63	D
5	598647.92	871571.91	1.98	221	2.131089	0.151089	49	E

6	598894.37	871549.26	1.36	316	1.39193	0.03193	55	F
7	598913.59	871565.25	1.44	326	1.600219	0.160219	51	G
8	598907.31	871690.09	4.73	353	4.792698	0.062698	63	H
9	599070.59	871728.35	2.69	411	2.699903	0.009903	49	I
10	599176.59	872109.15	2.32	540	2.194224	-0.12578	54	J
11	599256.52	872013.05	4.04	545	3.947141	-0.09286	63	K
12	599374.9	871948.91	2.54	577	2.476831	-0.06317	63	L
13	599250.24	872137.89	2.29	582	2.198883	-0.09112	54	M
14	599378.13	871984.12	2.88	590	2.845449	-0.03455	63	N
15	599285.45	872134.65	2.66	597	2.672002	0.012002	59	O
16	599496.5	871919.99	1.39	626	1.401585	0.011585	63	P
17	599375.08	872144.17	3.37	658	3.378542	0.008542	63	Q
18	599349.58	872253.03	0.68	696	0.882848	0.202848	47	R
19	599397.54	872195.36	3.28	699	3.234066	-0.04593	59	S
20	599448.73	872172.91	3.6	722	3.263684	-0.33632	63	T
21	599404.01	872265.78	2.29	738	2.189311	-0.10069	49	U
22	599602.31	872105.54	1.76	788	1.802842	0.042842	63	V
23	599685.48	872044.64	0.97	811	0.954024	-0.01598	58	W
24	599464.91	872348.94	2.07	816	2.43452	0.36452	48	X
25	599548.07	872288.04	2.36	840	2.348434	-0.01157	63	Y
26	599634.47	872262.35	1.6	874	1.516086	-0.08391	63	Z
27	599685.67	872239.9	1.89	892	1.956861	0.066861	63	AB
28	599612.21	872406.42	3.82	916	3.702656	-0.11734	63	AC
29	599807.27	872210.97	2.73	943	2.212384	-0.51762	51	AD
30	599813.74	872281.38	2.63	978	2.710474	0.080474	63	AE
31	599625.15	872547.24	2.18	986	1.997007	-0.18299	55	AF
32	599657.12	872508.8	2.69	988	2.713732	0.023732	63	AG
33	599791.48	872425.45	2.98	1036	2.976499	-0.0035	63	AH
34	599887.39	872310.12	2.98	1042	2.968437	-0.01156	53	AI
35	599903.38	872290.9	2.83	1043	2.528158	-0.30184	49	AJ
36	599650.84	872633.64	1.01	1045	1.064562	0.054562	48	AK
37	599714.78	872556.76	2.21	1049	2.153212	-0.05679	63	AL
38	599861.89	872418.98	2.47	1075	2.349999	-0.12	63	AM
39	599826.87	872617.47	2.32	1125	2.367422	0.047422	63	AN
40	599945.25	872553.34	1.74	1148	1.543708	-0.19629	50	AO
41	599916.51	872626.98	3.76	1153	3.162089	-0.59791	63	AP
42	600012.61	872706.91	3.33	1199	3.425309	0.095309	59	AQ
43	600054.29	872774.09	2.31	1223	2.399455	0.089455	61	AR
44	600188.84	872886.00	2.53	1274	2.458669	-0.07133	53	AS
45	600323.39	872997.90	2.96	1321	2.577318	-0.38268	46	AT
46	600483.62	873196.20	1.95	1363	2.01055	0.06055	53	AU
47	600675.65	873160.80	2.55	1398	2.448453	-0.10155	49	AV
48	600710.85	873157.57	1.65	1407	1.937697	0.287697	47	AW
49	600644.05	873589.76	1.61	1458	1.858565	0.248565	47	AX
50	600826.56	873644.00	2.23	1475	2.024403	-0.2056	30	AY
Root mean square error						0.18322392869677		

Note: The first three values are the X, Y and Z values from the original data file of each validation point. The next column (fifth column), titled ID is the line number from the original data file of the validation point. The next two columns are the estimated and residual values. The nData column contains the total number of original data points while the ID Label represents the alphabets assigned to each selected point.
The cross-validation data can be classified into three categories: the most underestimated data (i.e., data points for which the model's predictions consistently fall below the actual values), normally estimated data, and the most overestimated data (i.e., data points for which the model's predictions consistently exceed the actual values). However, the most under-estimated and most estimated data are outlined as follows.
Most under-estimated data:

X = 599916.51 Y = 872626.98 Z = 3.76

E = 3.1620894464873 ID = 1153

Most over-estimated data:

X = 599464.91 Y = 872348.94 Z = 2.07

E = 2.4345199697597 ID = 816

This test provided a quantitative measure of how well the grid file corresponds with the original bathymetric data file. The bathymetric charts, displaying points identification numbers and gridded depths to support Table 2, were subsequently produced (refer to Fig. 4a and 4b).

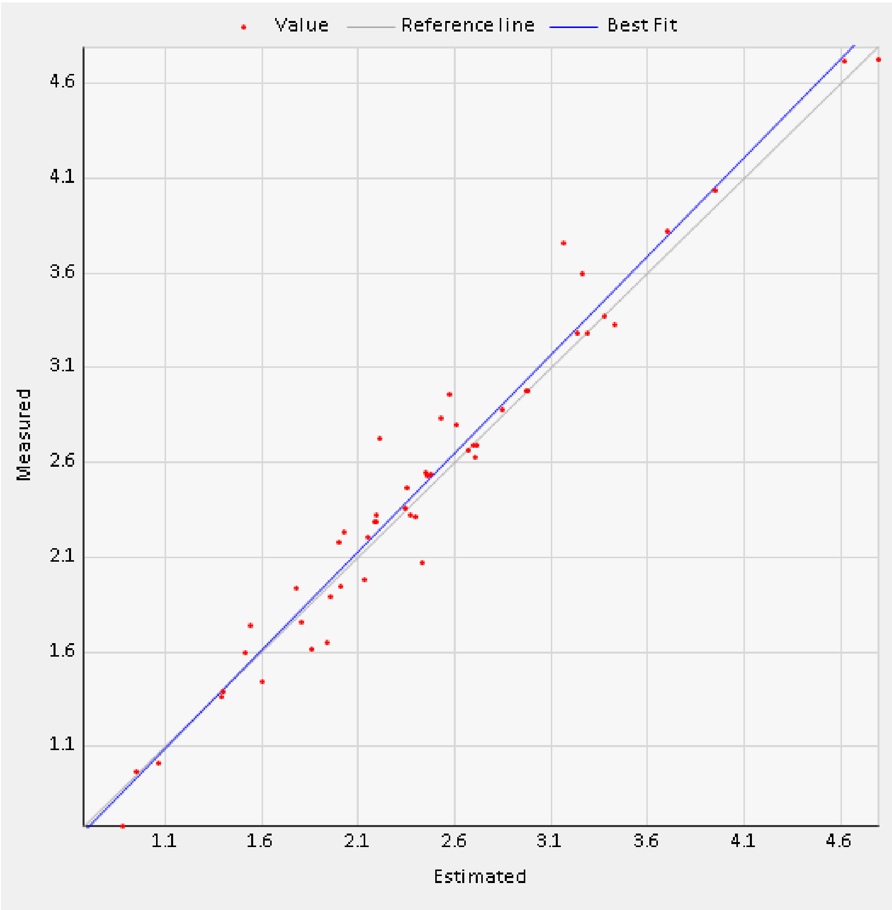

Fig. 4a: Cross validation generated profile

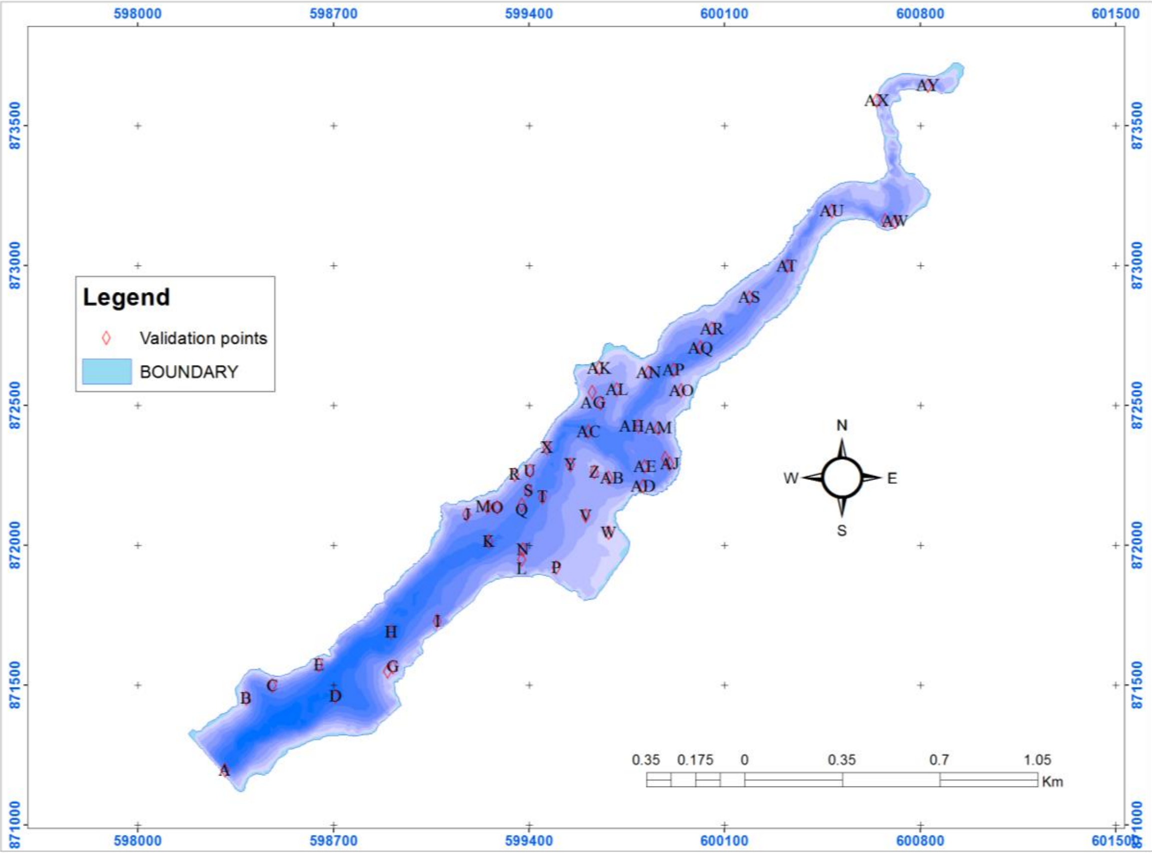

Fig. 4b: Cross validation points

2.2.3.5 Data processing with Hypack, ArcMap and Surfer

The study area's contour map, 3D surface map, and Flow direction map were produced using Surfer 16 software after the gridded data file passed the cross-validation test. Necessary geodetic and cartographic settings were also configured in the Hypack 2018 software to accurately plot sounding points. The sorted and/or rectified xyz data were imported and organized into a grid with 25-meter intervals, while the depth values were positioned following International Hydrographic Organization (IHO) standards. The final data was exported in Shapefile (.shp), AutoCAD (.dwg), and xyz data (.xyz) formats and then taken to ArcMap 10.5.1 for the creation of a Digital Depth Model (DDM) to display the depth variations for the different sounding points.

3. Results

The data collected from the sounding operation conducted between February 24th, 2022 and March 2nd, 2022 was utilized to create a 3D digital model representing the depth of the riverbed (Fig. 5) subsequent to the completion of aforementioned assessments. Different shades of blue were used to illustrate variations in depth, with deep blues indicating greater depth and light blues representing shallower areas. This is similar to a topographic digital elevation model (DEM) but specifically for underwater terrain, known as a digital depth model (DDM).

Isobaths (Fig. 6), a 3D surface representation (Fig. 7), and a map depicting peaks and depressions along with the flow direction (Fig. 8) of the surveyed area were generated using Surfer 16 software. These visuals showcase depth variations using a colour scale for better visualization. Deep blue signifies the deepest parts of the water, while areas toward the middle of the course are a mix of light and deep blue, and the shoreline and its surroundings are depicted in light blue. Additionally, a summary of the areas and volume data can be found in Table 4.

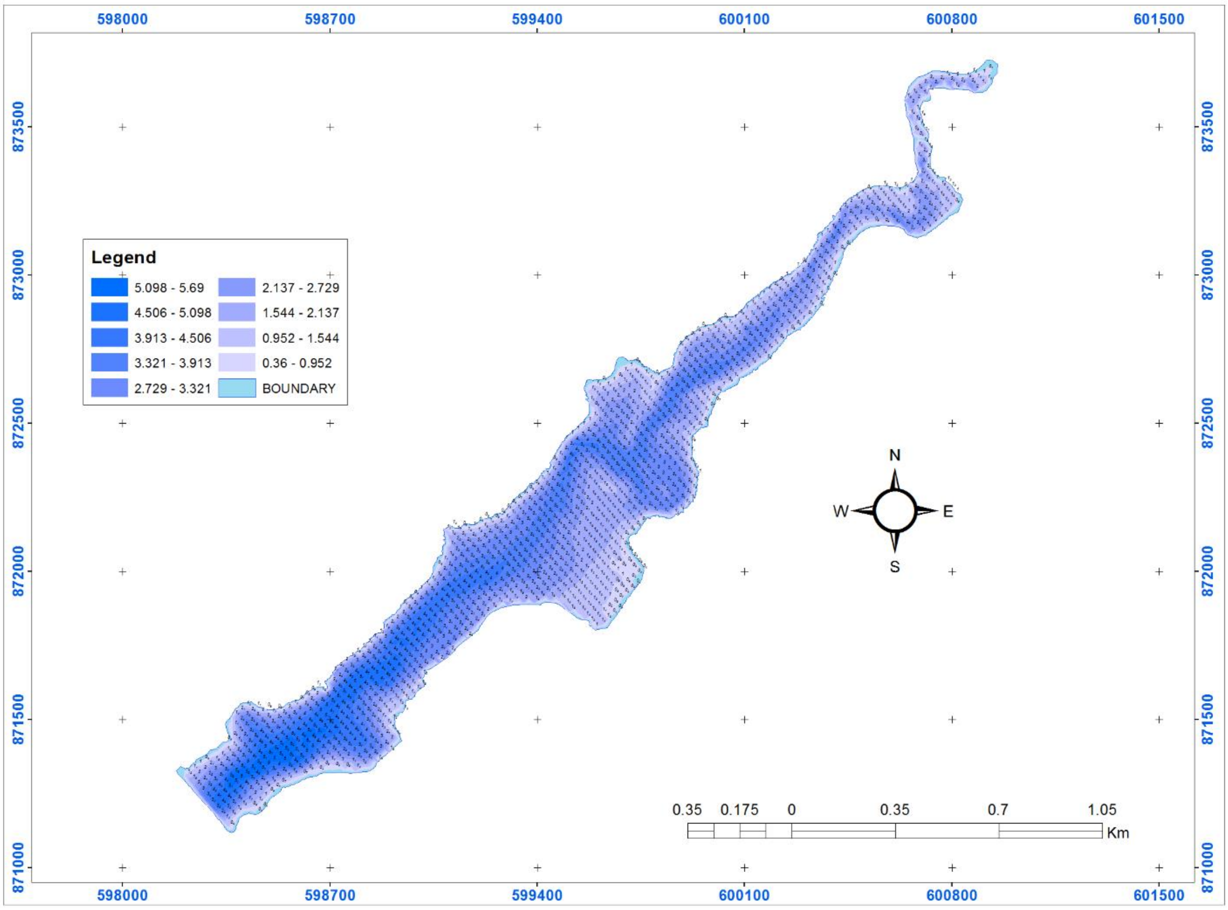

Fig. 5: Digital depth model

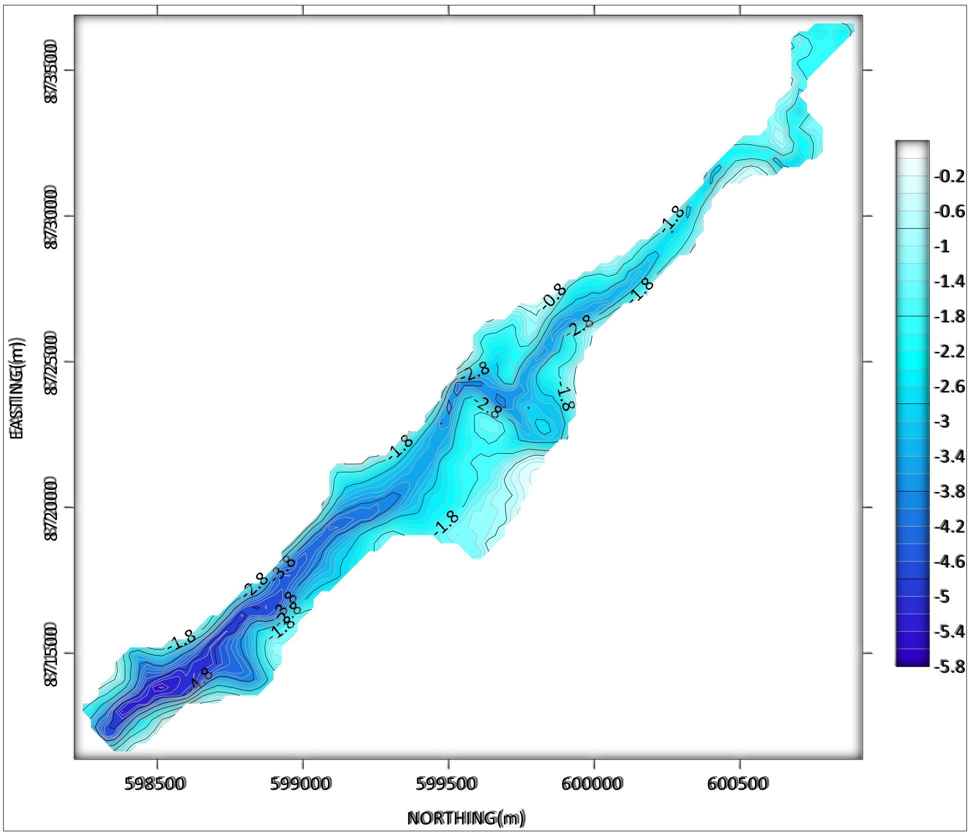

Fig. 6: Isobaths map of the reservoir

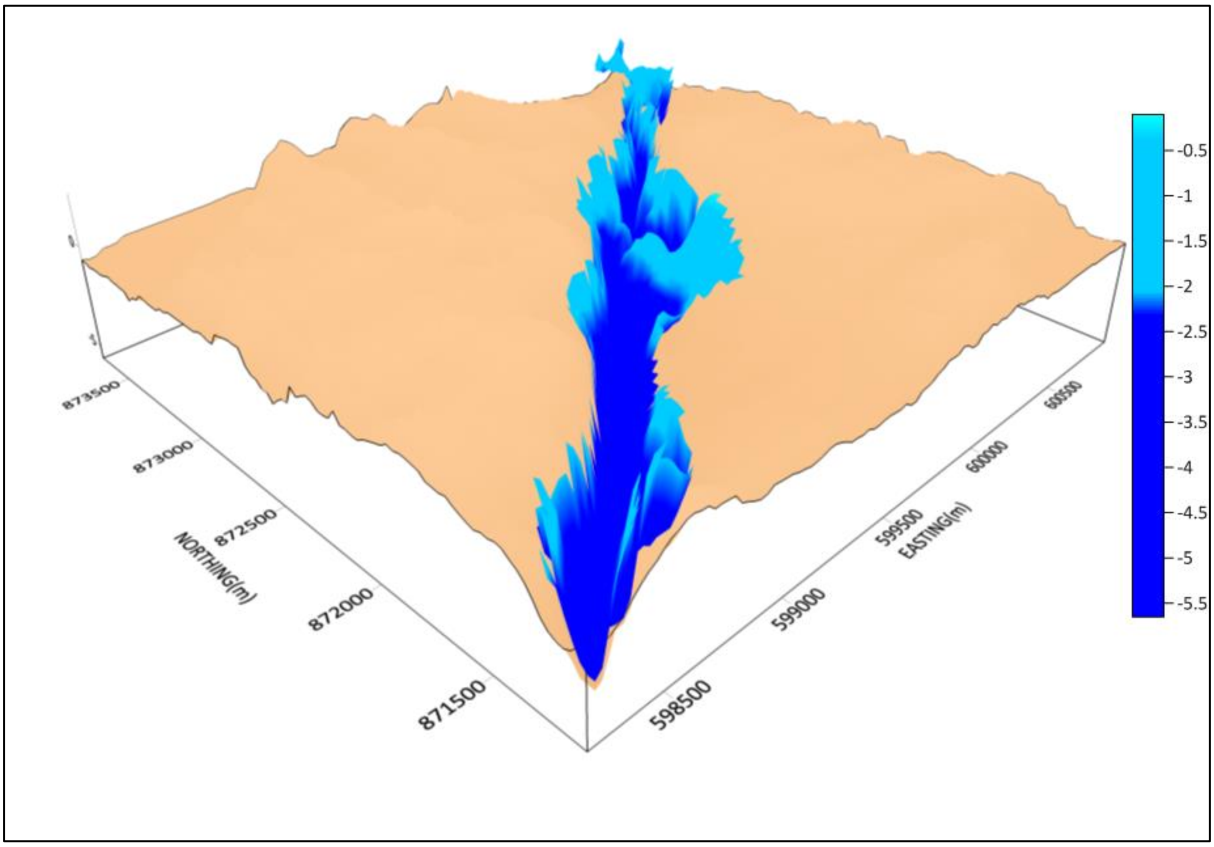

Fig. 7: 3D surface of Erelu reservoir

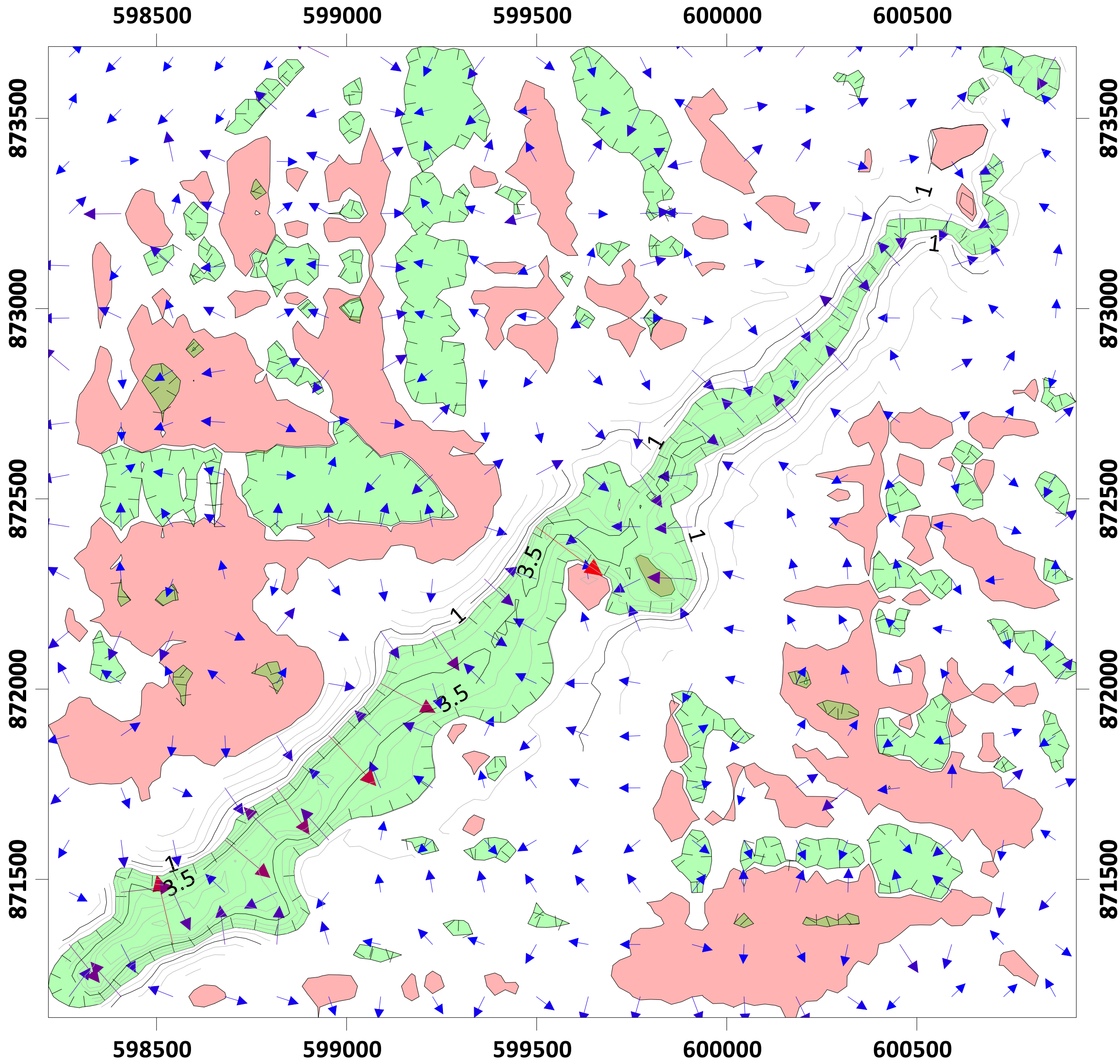

Fig. 8: Flow direction map (Peaks and depressions)

A peaks and depressions map create polygons around peaks and depressions in a grid file. These polygons represent the first or last closed polygon around an area where drainage flows away from it (peak) or into it (depression). In this peaks and depressions map, green areas depict depressions around the reservoir, red areas depict peaks around the reservoir, and areas with no colour depict terrain nearly at the same level as the shoreline. Fig. 8 shows that the waterbody itself falls under depression because water flows into it due to the nature of the surrounding terrain. The flow direction also indicates that any potential water flow is directed towards the waterbody. While this has some advantages, there are likely to be more disadvantages than advantages.

Table 4: Surface area and volume calculations

Description	Values
Maximum depth	5.69 m
Minimum Depth	0.36 m
Plane Height	0.00m (Water surface)
Height	Below plane height
Surface Area	$\approx$ 95 *hectare*
Volume	2,262,783.486m^3
Computed Average Depth	2.52 m

The depth ranges were categorised into three (Fig. 9) while area covered by each section and the percentage were summarized in Table 5 and analysed statistically in Fig. 10.

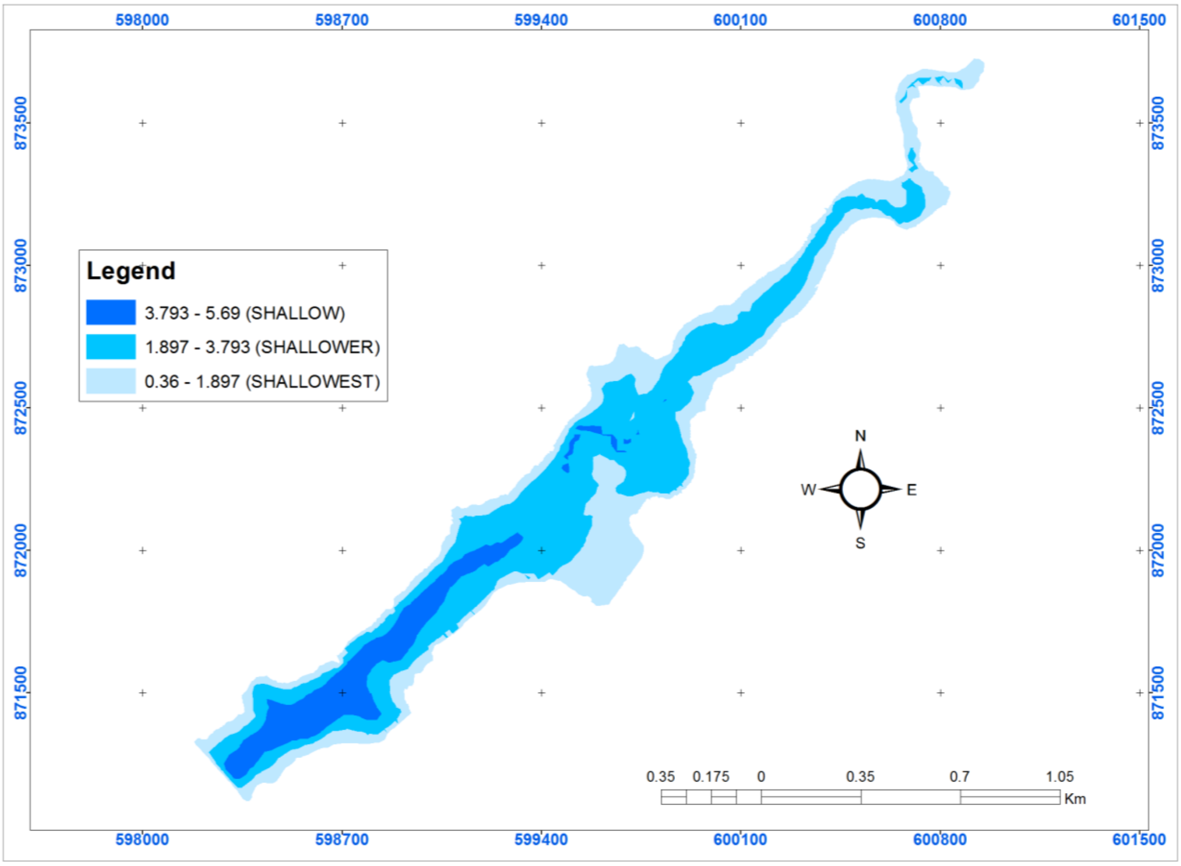

Fig. 9: Depth categories of the study area

Table 5: Summary of depth categories

Category	Area (m^2)	Area (Ha)	Area (%)
Shallow	117,653.967	11.7653967	12.40973559
Shallower	411,464.066	41.1464066	43.39981382
Shallowest	418,959.919	41.8959919	44.1904506
Total	948,077.952	94.808	100

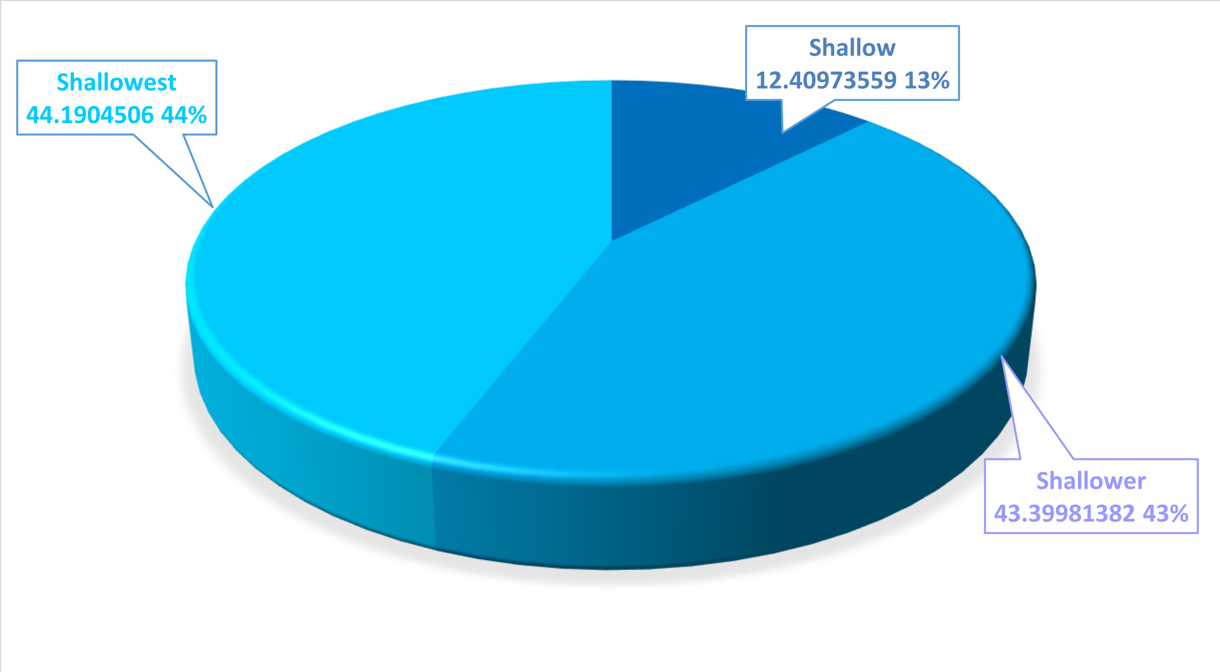

Fig. 10: Percentage covered by each category

4. Discussion

The data collected from monitoring the daily seasonal variation of the reservoir indicate no significant change in water level (refer to Appendix 1), suggesting that the Erelu reservoir is non-tidal. The final depth data revealed irregular depth values in certain areas due to uneven riverbeds, possibly caused by natural or human-related factors. Additionally, it was noted that the maximum depth of the study area is less than 6m, classifying the Erelu reservoir as shallow water. Consequently, the area was divided into three categories (see Fig. 9): shallow, shallower, and shallowest. The depth of the shallow area (depicted in deep blue) ranges from 3.79m to 5.69m, while the shallower part (in blue) ranges from 1.89m to 3.79m, and the shallowest part (in light blue) ranges from 0.36m to 1.90m. The extent of coverage for each category both in metric values and percentages were presented to support the detailed depth category map in Fig. 9 (see Table 5 and Fig. 10).

The reservoir cannot be constructed with this depth irregularity, so the shallower and shallowest areas need severe dredging. It can be observed that the deeper part of the reservoir falls in the middle, with the depth decreasing towards the shoreline, which calls for monitoring the reservoir's shoreline. The Isobaths map shows the elevation of all depths in the study area; the deep blue colour represents the reservoir coverage area. This is also evident on the 3D surface map where the shoreline and its surroundings are shown and represented with different shades of terrain colour. The water flow direction (Fig. 8) reveals continuous flow of water through the southwestern part of the waterbody.

Overall, the volume of the study area yields a total of 2,262,783.486m^3 for Erelu reservoir. However, this may not be enough for the populace of Oyo town using the 2006 population as a benchmark, though further research is needed to ascertain this claim. The calculated area of approximately 95ha is less than the area (161.07ha) recorded by some authors (Falaye et al., 2015; Kareem et al., 2018; Popoola et al., 2019). It can therefore be concluded that almost 67ha of the reservoir has been covered by aquatic weeds and other sediments, being used as farmlands, especially those close to the shore. Consequently, there is a need to clear the aquatic weeds and reclaim the farming areas, converting them back to reservoir to promote sustainability.

5. Conclusion

In this study, bathymetric mapping of the Erelu reservoir was conducted using a Single-beam Echosounder. The mapping provided sufficient seabed information, revealing depths ranging from 0.36m to 5.69m within the studied area. This indicates that the reservoir has a relatively shallow average depth of about 2.52m. Despite the flow from tributaries, the water level has not surpassed 0.5m above the recorded maximum since the observations, although it could reach up to 1.0m in the event of persistent rainfall. Therefore, there is an urgent need for complete dredging of the reservoir.

Funding

The authors did not receive support from any organization for the submitted work.

Credit Authorship Contribution Statement

Ibrahim Opeyemi Shittu: Supervision, Conceptualization, Methodology, Data analysis, Manuscript writing, Reviewing, Editing and Coordination of the research. Habeebullahi Oloyede Olorunkosebi: Methodology, Data Curation, Satellite data analysis, Manuscript writing, Reviewing, and Editing. Isa Adekunle Hamid-Mosaku: Conceptualization, Methodology, Data analysis, Reviewing, and Editing. Olalekan Abeeb Jimoh: Methodology, Data Curation, and Analysis. Olabamiji Mohammed Akindiya: Methodology, Data Curation, and Analysis. Latifat Olaide Oyelakin: Methodology, Data Curation, and Analysis. Luqman Obasekore Muhammed: Methodology, Data Curation, and Analysis. Kazeem Adewunmi Raheem: Methodology, Data Curation, and Analysis.

Declaration of competing interests

None. The authors declare that they have no known competing financial interests or personal relationships that could have appeared to influence the work reported in this paper.

Acknowledgements

The authors wish to acknowledge the support for the participant in this study and the anonymous experts and respondents, colleagues, and anonymous reviewers.

References

Alademomi, A.S. (2017) Morphodynamics in the Lagos Lagoon: Observation and Inferences of Change [PhD degree, University of Plymouth, Unpublished].

Ayoola, S.O. and Ajani, E.K. (2009) Seasonal variation in fish distribution and physicochemical parameters of wetland areas in Oyo State, Nigeria. International Journal Biological Chemical Sciences, 3: 107-116.

Badejo, O.T. and Adewuyi, G.K. (2019) Bathymetric Survey and Topography Changes Investigation of Part of Badagry Creek and Yewa River, Lagos State, Southwest Nigeria. Journal of Geography, Environment and Earth Science International, 22(4): 1-16.

Basson, G.R. (2009) Management of siltation in existing and new reservoirs. General Report. 89. Proc. of the 23rd Congress of the Int. Commission on Large Dams CIGBICOLD (vol. 2) Conf. 51-52.

Breman, J. and Kearns, T.A. (2010) Bathymetry - the art and science of seafloor modeling for modern applications. ESRI International Underwater Explorations, 1-36.

Dierssen, H.M. (2014) Bathymetry: Assessing Methods. Encyclopedia of Natural Resources.

Dierssen, H.M. and Randolph, K. (2011) Encyclopedia of sustainability science and technology, Springer. In.

Elhassan, I. (2015) Bathymetric techniques. International Federation of Surveyors (FIG), FIG Working Week, Sofia, Bulgaria.

Falaye, A.E., Ajani, E.K., Kareem, O.K. and Olanrewaju, A.N. (2015) Assessment of Ichthyofaunal assemblage of Erelu Reservoir, Oyo, Nigeria. Journal of Ecologia, 5(2): 43-53.

FIG (International Federation of Surveyors) Commission 4. Working Group Hydrographic Surveying in Practice (2010) Guidelines for the Planning, Execution and Management of Hydrographic Surveys in Ports and Harbours. International Federation of Surveyors (FIG).

Jenyo-Oni, A., Hassan, A.A. and Dauda, A.B. (2014) Investigation of biological condition of fish species in lower Ogun River wetlands, Lag os, Nig eria. International Journal of Biological and Chemical Sciences, 8(2): 705-710.

Kareem, O.K. (2016) Thesis.Ecological evaluation and sustainable fish production in Erelu reservoir, Oyo, Nigeria. University of Ibadan, Nigeria.

Kareem, O.K., Ajani, E.K., Omitoyin, B.O., Olanrewaju, A.N., Orisasona, O. and Osho, E.F. (2018) Spatial and temporal limnological status of Erelu Reservoir, southwestern Nigeria. Ife Journal of Science, 20(3): 509-518.

Kareem, O.K., Olanrewaju, A.N. and Orisasona, O. (2015) Length-weight relationship and condition factor of Chrysichythys nigrodigitatus and Schilbe mystus in Erelu Lake, Oyo State, Nigeria. Journal of Fisheries and Livestock Production, 3(4): 1-4.

Kim, H.D., Aoki, S.I., Kim, K.H., Kim, J., Shin, B.S. and Lee, K. (2020) Bathymetric Survey for Seabed Topography using Multibeam Echo Sounder in Wando, Korea. Journal of Coastal Research, 95(SI): 527-531.

Kopacz, Z., Morgas, W. and Urbanski, J. (1996) The Hydroraphic Information, its Properties, Processing and Use. . International Hydrographic Review, 1: 27-40.

Le Deunf, J., Debese, N., Schmitt, T. and Billot, R. (2020) A review of data cleaning approaches in a hydrographic framework with a focus on bathymetric multibeam echosounder datasets. Geosciences, 10(7):254.

NOAA. (2021). National Oceanic and Atmospheric Administration. Significance of bathymetry surveying. Retrieved March, 3rd from https://oceanservice.noaa.gov/facts/eutrophication.html

Ojinnaka, O.C. (2007) Principles of hydrographic surveying - form sextant to satellite. El' Demak Publishers.

Olanrewaju, A.N., Ajani, E.K. and Kareem, O.K. (2017) Physico-chemical status of Eleyele Reservoir, Ibadan, Nigeria. Journal of Aquaculture Resources and Development, 8(9):512.

Popoola, K., Sowunmi, A. and Amusat, A. (2019) Comparative study of physico-chemical parameters with national and international standard and the insect community of Erelu Reservoir in Oyo town, Oyo State, Nigeria. International Journal of Water Resources and Environmental Engineering, 11(3): 56-65.

Rahmani, V., Kasten, J.H., DeNoyelles, F., Jakubauskas, M.E., Martinko, E.A., Huggins, D.H. (2018) Examining Storage Capacity loss and Sedimentation rate of Large Reservoirs in the Central US Great Plains. Water, 10(2):190.

Šiljeg, A., Marić, I., Domazetović, F., Cukrov, N., Lovrić, M. and Panđa, L. (2022) Bathymetric Survey of the St. Anthony Channel (Croatia) Using Multibeam Echosounders (MBES)—A New Methodological Semi-Automatic Approach of Point Cloud PostProcessing. Journal of Marine Science and Engineering, 10(1):101.

Ugwu, S.J., Ajoge, H.N., Abdulsalam, B. and Nwude, M.O. (2021) Bathymetry Study of the Siltation Level of Lugu Dam Reservoir in Sokoto State, Nigeria. Nigerian Journal of Technological Development, 18(3): 238-243.

Appendix 1: Tidal reading (in meters)

Day 1

S/N	Time	Staff reading	Range
1	11:23 am	0.57	0
2	11:33 am	0.57	0
3	11:43 am	0.57	0
4	11:53 am	0.57	0
5	12:03 pm	0.57	0
6	12:13 pm	0.572	0.002
7	12:23 pm	0.57	(-)0.002
8	12:33 pm	0.571	0.001
9	12:23 pm	0.57	(-)0.001
10	12:53 pm	0.573	0.003
11	1:03 pm	0.57	(-)0.003
12	1:13 pm	0.57	0
13	1:23 pm	0.572	0.002
14	1:33 pm	0.57	(-)0.002
15	1:43 pm	0.57	0
16	1:53 pm	0.57	0
17	2:03 pm	0.573	0.003
18	2:13 pm	0.57	(-)0.003

Day 2

S/N	Time	Staff reading	Range
1	11:00 am	0.472	0
2	11:10 am	0.473	0.001
3	11:20 am	0.471	(-)0.002
4	11:30 am	0.473	0.002
5	11:40 am	0.472	(-)0.001
6	11:50 am	0.473	0.001
7	12:00 pm	0.471	(-)0.002
8	12:10 pm	0.471	0
9	12:20 pm	0.473	0.002
10	12:30 pm	0.473	0
11	12:40 pm	0.473	0
12	12:50 pm	0.473	0
13	1:00 pm	0.472	(-)0.001
14	1:10 pm	0.472	0
15	1:20 pm	0.473	0.001
16	1:30 pm	0.473	0
17	1:40 pm	0.473	0
18	1:50 pm	0.473	0
19	2:00 pm	0.473	0
20	2:10 pm	0.473	0
21	2:20 pm	0.474	0.001
22	2:30 pm	0.474	0
23	2:40 pm	0.473	(-)0.001
24	2:50 pm	0.473	0
25	3:00 pm	0.473	0
26	3:10 pm	0.473	0
27	3:20 pm	0.473	0
28	3:30 pm	0.473	0

29	3:40 pm	0.472	(-)0.001
30	3:50 pm	0.473	0.001
31	4:00 pm	0.473	0

DAY 3			
S/ N	Time	Staff reading	Range
1	10:24 am	0.483	0
2	10:34 am	0.482	(-)0.001
3	10:44 am	0.482	0
4	10:54 am	0.484	0.002
5	11:04 am	0.483	(-)0.001
6	11:14 am	0.482	(-)0.001
7	11:24 am	0.483	0.001
8	11:34 am	0.483	0
9	11:44 am	0.483	0
10	11:54 am	0.484	0.001
11	12:04 pm	0.484	0
12	12:14 pm	0.483	(-)0.001
13	12:24 pm	0.483	0
14	12:34 pm	0.483	0
15	12:44 pm	0.485	0.002
16	12:54 pm	0.482	(-)0.003
17	1:04 pm	0.482	0
18	1:14 pm	0.483	0.001
19	1:24 pm	0.483	0
20	1:34 pm	0.483	0
21	1:44 pm	0.482	(-)0.001
22	1:54 pm	0.483	0.001
23	2:04 pm	0.483	0
24	2:14 pm	0.483	0
25	2:24 pm	0.482	(-)0.001

DAY 4			
S/N	Time	Staff reading	Range
1	10:47 am	0.586	
2	10:57 am	0.586	0
3	11:07 am	0.587	0.001
4	11:17 am	0.588	0.001
5	11:27 am	0.587	(-)0.001
6	11:37 am	0.587	0
7	11:47 am	0.586	(-)0.001
8	11:57 am	0.586	0
9	12:07 pm	0.587	0.001
10	12:17 pm	0.587	0
11	12:27 pm	0.588	0.001
12	12:37 pm	0.588	0
13	12:47 pm	0.587	(-)0.001
14	12:57 pm	0.588	0.001
15	1:07 pm	0.588	0
16	1:17 pm	0.587	(-)0.001
17	1:27 pm	0.586	(-)0.001
18	1:37 pm	0.587	0.001
19	1:47 pm	0.587	0
20	1:57 pm	0.587	0
21	2:07 pm	0.587	0
22	2:17 pm	0.586	(-)0.001
23	2:27 pm	0.587	0.001
24	2:37 pm	0.588	0.001
25	2:47 pm	0.586	(-)0.002
26	2:57 pm	0.586	0
27	3:07 pm	0.587	0.001
28	3:17 pm	0.586	(-)0.001
29	3:27 pm	0.587	0.001
30	3:37 pm	0.588	0.001
31	3:47 pm	0.588	0
32	3:57 pm	0.587	(-)0.001
33	4:07 pm	0.587	0
34	4:17 pm	0.588	0.001

Day 5			
S/N	Time	Staff reading	Range
1	10:50 am	0.5	0
2	11:00 am	0.5	0
3	11:10 am	0.499	(-)0.001
4	11:20 am	0.499	0
5	11:30 am	0.499	0
6	11:40 am	0.499	0
7	11:50 am	0.5	0.001
8	12:00 pm	0.5	0
9	12:10 pm	0.5	0
10	12:20 pm	0.5	0
11	12:30 pm	0.5	0
12	12:40 pm	0.5	0
13	12:50 pm	0.5	0
14	1:00 pm	0.5	0

15	1:10 pm	0.5	0
16	1:20 pm	0.5	0
17	1:30 pm	0.5	0
18	1:40 pm	0.5	0
19	1:50 pm	0.5	0
20	2:00 pm	0.5	0
21	2:10 pm	0.5	0
22	2:20 pm	0.5	0
23	2:30 pm	0.5	0
24	2:40 pm	0.5	0
25	2:50 pm	0.5	0
26	3:00 pm	0.5	0
27	3:10 pm	0.5	0
28	3:20 pm	0.5	0
29	3:30 pm	0.5	0
30	3:40 pm	0.5	0

Day 6			
S/N	Time	Staff reading	Range
1	1:30 pm	0.45	0
2	1:40 pm	0.45	0
3	1:50 pm	0.45	0
4	2:00 pm	0.45	0
5	2:10 pm	0.45	0
6	2:20 pm	0.45	0
7	2:30 pm	0.45	0
8	2:40 pm	0.45	0
9	2:50 pm	0.45	0
10	3:00 pm	0.45	0
11	3:10 pm	0.45	0
12	3:20 pm	0.47	0.02
13	3:30 pm	0.47	0
14	3:40 pm	0.47	0
15	3:50 pm	0.47	0
16	4:00 pm	0.47	0
17	4:10 pm	0.472	0.002
18	4:20 pm	0.472	0
19	4:30 pm	0.472	0
20	4:40 pm	0.472	0
21	4:50 pm	0.472	0
22	5:00 pm	0.472	0
23	5:10 pm	0.472	0

Appendix 2: Minimum Bathymetry Standards for Safety of Navigation Hydrographic Surveys

Criteria	Order 2	Order 1b	Order 1a	Special Order	Exclusive Order
Area description (Generally)	Areas where a general description of the sea floor is considered adequate.	Areas where underkeel clearance is not considered to be an issue for the type of surface shipping expected to transit the area.	Areas where underkeel clearance is considered not to be critical but features of concern to surface shipping may exist.	Areas where underkeel clearance is critical	Areas where there is strict minimum underkeel clearance and manoeuvrability criteria
Depth THU [m] + [% of Depth]	20 m + 10% of depth	5 m + 5% of depth	5 m + 5% of depth	2 m	1 m
Depth TVU	a = 1.0m b = 0.023	a = 0.5 m b = 0.013	a = 0.5 m b = 0.013	a = 0.25 m b = 0.0075	a = 0.15 m b =0.0075
Feature Detection [m] or [% of Depth]	Not Specified	Not Specified	Cubic features > 2 m, in depths down to 40 m; 10% of depth beyond 40 m	Cubic features > 1 m	Cubic features > 0.5 m
Feature Search [%]	Recommended but Not Required	Recommended but Not Required	100%	100%	200%
Bathymetric coverage [%]	5%	5%	≤ 100%	100%	200%

Note: Safety of navigation survey standards (as defined in Appendix 2) are referenced to the Matrix criteria (available in IHO-S44 Standards Manual Sixth Edition). However, the range of accuracies presented in the Matrix was designed to accommodate other surveys (e.g. geophysical, oil and gas, dredging, and geotechnical) to provide a common framework for tasking and assessing hydrographic surveys in general.